Compositional Characterization of Pyrolysis Fuel Oil from Naphtha and Vacuum Gas Oil

AUTHORS' NAMES: Nenad D. Ristic[1], Marko R. Djokic[1], Elisabeth Delbeke[1,2], Arturo Gonzalez-Quiroga[1], Christian V. Stevens[2], Kevin M. Van Geem[1], Guy B. Marin[1]

AUTHORS' ADDRESS:

1. Laboratory for Chemical Technology, Ghent University, Technologiepark 914, 9052 Ghent, Belgium.

2. SynBioC, Deparmtent of Sustainable Organic Chemistry and Technology, Ghent University, Coupure Links 653, 9000 Ghent, Belgium.

KEYWORDS: Steam Cracking, PAH, Aromatic hydrocarbons, NMR, GC × GC – FID/TOF-MS.

ABSTRACT

Steam cracking of crude oil fractions gives rise to substantial amounts of a heavy liquid product referred to as Pyrolysis Fuel Oil (PFO). To evaluate the potential use of PFO for production of value-added chemicals a better understanding of the composition is needed. Therefore, two PFO's derived from naphtha (N-PFO) and Vacuum Gas Oil (V-PFO) were characterized using elemental analysis, SARA fractionation, nuclear magnetic resonance (NMR) spectroscopy and

comprehensive two-dimensional gas chromatography (GC × GC) coupled to a flame ionization detector (FID) and time-of-flight mass spectrometer (TOF-MS). Both samples are highly aromatic, with molar hydrogen-to-carbon (H/C) ratios lower than 1 and with significant content of compounds with solubility characteristics typical for asphaltenes and coke, *i.e.* n-hexane insolubles. The molar H/C ratio of V-PFO is lower than the one measured for N-PFO, as expected from the lower molar H/C ratio of the VGO. On the other hand, the content of n-hexane insolubles is lower in V-PFO compared to the one in N-PFO, *i.e.* 10.3 ± 0.2 wt.% and 19.5 ± 0.5 wt.%, respectively. This difference is attributed to the higher reaction temperature applied during naphtha steam cracking, which promotes the formation of poly-aromatic cores and at the same time scission of aliphatic chains. The higher concentrations of purely aromatic molecules present in N-PFO is confirmed via NMR and GC × GC – FID/TOFMS. The dominant chemical family in both samples are diaromatics, with a concentration of 28.6 ± 0.1 wt.% and 27.8 ± 0.1 wt.% for N-PFO and V-PFO, respectively. Therefore, extraction of valuable chemical industry precursors such as diaromatics and specifically naphthalene is considered as a potential valorization route. On the other hand, hydro-conversion is required to improve the quality of the PFO's before exploiting them as a commercial fuel.

1. INTRODUCTION

Steam cracking is considered as one of the most important petrochemical processes due to its predominance for the production of light olefins such as ethylene and propylene[1]. In the steam cracking process saturated hydrocarbons are broken down into smaller, mainly unsaturated, hydrocarbons in a coil constructed of high-temperature resistant alloys suspended in the radiant reactor of a gas fired furnace. Subsequently, the product stream is cooled down in the transfer

line heat exchanger (TLE), to minimize unwanted reactions of valuable products such as ethylene, propylene and butadiene. Ethane, liquefied petroleum gas and naphtha are typically used as feedstocks for steam cracking. Nevertheless, heavier feedstocks such as atmospheric and vacuum gas oils (VGO) are possible alternatives. Compared to lighter feedstocks, steam cracking of high-boiling point mixtures results in lower yields of light olefins, higher yields of steam cracking by-products and higher fouling rates in the reactor and the TLE[2-4]. While pyrolysis gasoline, containing primarily benzene, toluene and xylene, is straightforward to valorize, the heavier by-products called steam cracking residue or pyrolysis fuel oil (PFO) are more difficult to exploit. PFO, separated from valuable products via primary fractionation, is rich in poly-aromatic molecules[5, 6] which makes it attractive for the production of carbon black[7] and for naphthalene extraction[8]. More often, heavy PFO is used for blending and subsequently as an industrial fuel, flux oil or bunker fuel. Depending on the feedstock and steam cracking severity, the impact of PFO on the overall ethylene plant economy can be significantly different. The amount produced varies considerably, *e.g.* 3.0-6.0 wt.% and 21.0-25.0 wt.% for naphtha and VGO, respectively[9]. Knowledge of the precise chemical composition is fundamental for assessing the valorization, integration possibilities, and the required downstream processing steps. Most importantly an improvement of the molecular characterization of heavy reaction products is a necessary step for optimization of the steam cracking process when heavy liquids are used. In other words, it is a pre-requirement before one could even attempt modelling of heavy hydrocarbon mixture pyrolysis[10]. Additionally, identification and quantification of heavy poly-aromatics is in particularly important for improving the understanding of coke formation during steam cracking of hydrocarbons. Heavy poly-aromatics are considered as some of the main coke precursors in both the reactor and the TLE of a steam cracker[11]. Moreover,

compositional characterization of the stream is a requirement for optimizing downstream processes. A recurrent problem is the gum formation via polymerization, which causes incomplete combustion when the stream is utilized as a fuel. Finally, environmental concerns drive the industry towards molecular characterization, since several compounds are highly carcinogenic[12].

Despite the increasing importance of compositional characterization promoted by so-called molecular based management[13, 14], methodologies employed by the mayor oil and petrochemical companies, detailed results for PFO are scarce or unavailable in open literature due to difficulties in performing experiments on relevant steam cracking conditions, producing sufficient sample quantities and challenging sample preparation procedures. Moreover, the poly-aromatic nature of the mixture requires the development of methods able to resolve the complicated PFO matrix. Fast scanning of heavy hydrocarbon mixtures, *i.e.* heavy crude oil, bitumen[15], sand oil[16] and even asphaltenes[17], can be achieved via Direct Insertion Probe-Mass Spectrometry (DIP-MS). Discrimination of heavy molecules is avoided by a program evaporation under vacuum conditions and direct transfer towards the MS. Therefore, the DIP-MS method enables finger-printing of samples and a rough separation based on volatility. Nevertheless, the separation resolution is limited and the quantification via MS is challenging due to an enormous calibration effort[18]. On the other hand, gas chromatography provides higher resolution for the characterization of poly-aromatic hydrocarbons[12, 19]. In particular comprehensive two-dimensional gas chromatography (GC × GC) is a superior characterization technique for characterization of petroleum-derived samples compared to one dimensional GC[20-23]. Dutriez et al.[24, 25] developed a GC × GC method for quantitative analysis of heavy hydrocarbons with carbon numbers up to C_{60}, and subsequently optimized the method to characterize vacuum resin

fractions without discrimination in the injector[26]. However, the detailed composition could not be obtained due to substantial co-elution of different compounds. On the other hand, Fourier Transform Ion Cyclotron Resonance Mass Spectrometry (FT-ICR-MS) showed that GC methods do not characterize all the heavy poly-aromatic compounds in coal tar[27]. Even though high resolution FT-ICR-MS enables accurate determination of the molecular mass and chemical nature of heavy compounds[28-30], accurate quantification remains a challenge[31, 32]. Complicated sample matrices can alternatively be analyzed via Nuclear Magnetic Resonance (NMR) spectroscopy, which provides information on the relative abundance of chemical families[33, 34]. Similarly, poly-aromatic compounds can be separated using liquid chromatography[35-38]; nevertheless, the developed methods are time consuming and still primarily qualitative. Due to the inherent limitations of each discussed analytical method only a combination of different analytical techniques can result in quantitative characterization of fractions such as PFO.

In this work we have for the first time characterized PFO samples produced during steam cracking of naphtha and VGO. Elemental analysis, SARA (saturates, aromatics, resins and asphaltenes) fractionation, NMR and GC × GC coupled with Time of Flight Mass Spectroscopy (TOF-MS) and Flame Ionization Detector (FID) allowed characterization and comparison between two potentially very different PFO samples. Finally, guidelines for further processing of heavy steam cracking products are given based on the performed detailed characterization.

2. EXPERIMENTAL SECTION

2.1. Chemicals

Analytical gases (helium, oxygen, nitrogen, hydrogen and air) used for elemental analysis and GC × GC have a minimal purity of 99.99% (Air Liquide, Belgium). 3-chlorothiophene, used as internal

standard in GC × GC analyses, has a purity of 98% (Sigma-Aldrich, Belgium). 2-chloropyridine, used as a secondary internal standard in GC × GC analyses has a purity of 99% (Sigma-Aldrich, Belgium). Carbon disulfide used as a solvent for GC × GC analyses was supplied with a 99.9% purity (Sigma-Aldrich, Belgium). The purity of deuterated chloroform, the solvent used for NMR analysis, is 99.8 % (Sigma-Aldrich, Belgium). A standard Poly-nuclear Aromatic Hydrocarbons (PAH) mixture supplied by Sigma-Aldrich (Belgium, CRM47543) was used for GC × GC method development. Dichloromethane (DCM) used for extraction of heavy organic reaction by-products was supplied with a 98% purity (Chem-Lab, Belgium). DCM and n-hexane used for SARA fractionation (Sigma-Aldrich, Belgium) are HPLC grade. Steam used as a diluent in cracking experiments was produced by superheating of water demineralized over an ion exchange column.

2.2. Steam cracking feedstocks

Two different crude oil fractions, naphtha and vacuum gas oil (VGO), were tested as steam cracking feedstocks. These feedstocks were provided by Total (Antwerp, Belgium) and some of their global characteristics are given in Table 1. The boiling point curve was determined using an ASTM D1160 distillation unit (B/R instruments, USA) at atmospheric pressure for naphtha and at a reduced pressure of 0.13 kPa for VGO. Elemental (CHNS & O) and PINA (paraffins, isoparaffins, naphthenes, aromatics) compositions were obtained using the method developed by Dijkmans et al.[39].

Table 1. Elemental composition, molecular family mass percentage and boiling point curve of naphtha and VGO.

2.3. Pilot plant steam cracking experiments

Steam cracking experiments were performed in the pilot plant steam cracker (Laboratory for Chemical Technology, Ghent University, Ghent, Belgium) which is described in detail elsewhere[40, 41]. An Incoloy 800HT reactor (12.8 m, 9 mm I.D.) is suspended in the gas-fired furnace divided into five separate cells, in which the temperature is independently controlled by regulating the fuel supply. Twenty thermocouples and five manometers are located along the reactor coil. The pilot plant effluent is sampled on-line at high temperature (673 K - 773 K) using a valve-based sampling system and an uniformly heated transfer line[40, 42]. Downstream, the steam cracking effluent enters the TLE from the top side and is cooled at controlled temperature. Namely, TLE temperature profile is controlled by regulating the flowrate of the co-currently fed cooling air and by setting the temperature in three independent heating zones.

Downstream of the TLE, the effluent stream is cooled to 353 K using an oil cooler heat exchanger. The gas stream containing the main reaction products, *i.e.* ethylene, propylene and butadiene, is send to the flare connected to the vent line. On the other hand, water and cracking by-products, PFO and a fraction of pyrolysis gasoline, are condensed and collected in a knock-out drum. Subsequently, the mixture is transferred into a sampling vessel via transfer line kept at 373 K in order to prevent solidification of heavy reaction products. The interested reader is referred to the Supplementary Information for a schematic description of the steam cracking pilot plant.

Naphtha was cracked at a coil outlet temperature of 1123 K, coil outlet pressure of 170 kPa, steam dilution ratio of 0.5 kg/kg. Conversely, VGO was cracked at a coil outlet temperature of 1073 K, coil outlet pressure of 170 kPa and steam dilution ratio of 1.0 kg/kg. For both cases the

TLE outlet temperature was kept at 673 K. These operating conditions are generally applied for cracking of similar feedstocks[2, 9, 10, 43].

2.4. Sample preparation procedure

Heavy reaction products, *i.e.* a collected mixture of pyrolysis gasoline, PFO and water (see section 2.3.), were mixed and transferred to three identical vessels with a volume of 1 L. In the following step, 200 mL of the mixture was mixed with 100 mL of DCM and kept for two hours in a 500 mL borosilicate glass separation funnel. After complete separation of the phases, the DCM extract was transferred to a 2 L collecting vessel. Subsequently, approximately 500 mL of the extract was transferred to a 1 L vessel connected to a rotary evaporator. The water residue, compounds with lower boiling point considered as pyrolysis gasoline and the solvent, *i.e.* DCM were evaporated at 353 K and 5 kPa. The obtained hydrocarbon residue is considered as the PFO sample.

2.5. Analytical Methods

2.5.1. Elemental analysis

Thermo Scientific™ FLASH 2000 Series Elemental Analyzer (EA) (Interscience, Belgium) equipped with a Thermal Conductivity Detector is used for determination of the elemental composition. The solid cup injection technique is chosen to avoid injection discrimination of PFO samples (see section 2.4.). The uncertainties on the detected amounts of carbon, hydrogen and oxygen were within vendor specifications. The elemental composition is based on three repeated analyses. The summations of CHNSO mass percentages were always within 97 and 103%.

2.5.2. SARA fractionation

Fractionation was initiated by keeping the PFO samples (see section 2.4.) under an 1 L min^{-1} nitrogen flow, temperature of 333 K and pressure of 5 kPa for 72 hours. The mass evaporated during that period was considered as a topping loss. After evaporation of all light compounds, n-hexane insolubles, further considered as asphaltenes and coke, precipitated from the rest of the hydrocarbon matrix. 210-250 mg of the sample was filtered after dissolving in 1 mL of n-hexane. Asphaltenes and coke were later removed from the filter by dissolving them in DCM. Subsequent separation of fractions referred to as saturates, aromatics and resins was performed on a mid-pressure liquid chromatography (MPLC) system (Köhnen-Willsch, Jülich, Germany). The dissolved fraction was injected into a pre-column filled with deactivated fine silica (63-200 μm) and deactivated coarse silica (200-500 μm). A flow of 2.4 mL min^{-1} of n-hexane was constantly fed to the pre-column for 450 s flushing the saturate and aromatic fractions into the main column. On the other hand, the resin fraction remained on the pre-column. Subsequently, saturate and aromatic fractions were separated in the main column filled with fine deactivated silica (40-63 μm) and the saturate fraction was collected after 180 s. Next, the pre-column was removed and the main column back-flushed for 450 s with an increased n-hexane flow of 3.0 ml min^{-1}, thus enabling the elution of the aromatic fraction. A Refractive Index Detector and Ultraviolet Detector were used to monitor the elution of the above-mentioned fractions. The resin fraction trapped on the silica packing of the pre-column was separated by dissolving it in DCM and filtering of the silica. Finally, saturate and aromatic fractions were placed in a vaporizer where at 303 K and air flow of 70 ml min^{-1} the majority of the n-hexane was removed. The residue was washed with DCM and transferred to a weighted vial. Each fraction was placed in

the fume hood over night to evaporate DCM. In the last step, the vials were weighted and the masses of each separated fraction determined.

2.5.3. NMR

100 mg of each PFO sample (see section 2.4.) was dissolved in 1 mL of $CDCl_3$ (deuterated chloroform) and filtered over cotton wool in a Pasteur pipette to remove all insoluble particles. The cotton wool was rinsed until becoming colorless with an additional 0.2 mL of $CDCl_3$, and the combined solvent fractions were dried under reduced pressure. The ^{13}C-NMR spectra are recorded on a 400 MHz NMR spectrometer (Bruker Avance III Nanobay) at a resonance frequency of 100 MHz using a 5 mm broadband probe. The solvent signal of 77.16 ppm is used as the internal reference. Using $CDCl_3$ as a solvent enables analyzing of the same sample via proton NMR if necessary and furthermore secures accurate chemical shift locking. The ^{13}C-NMR spectra is acquired with 30° pulse angle, proton decoupling, sweep width of 24038.461 Hz, and corresponding acquisition time of 1.36 s. Acquisition of 2048 scans using a 8 s pulse delay resulted in a good signal-to-noise ratio after 5.40 h of total time of measurement per sample. All experiments were performed at 298 K. The spectra were processed using TopSpin 3.2 to perform baseline corrections and integrations.

The NMR spectra are interpreted according to the methodology initially developed by Solum et al.[44] and later applied for kerogen characterization by Kelemen et al.[34]. However, the dipolar dephasing, which allows the separation of protonated and non-protonated aromatic carbons[34], was not possible and thus the fraction of bridgehead non-protonated aromatic carbon and average carbon number per aromatic were not calculated.

2.5.4. GC × GC

2.5.4.1. Sample preparation

Two samples of each PFO (see section 2.4) were prepared for analyses using GC × GC – FID, and GC × GC – TOF-MS. 3-chlorothiophene and 2–chloropyridine were chosen as internal standards for FID analysis. These internal standards were added to the PFO samples according to the procedure described by Dijkmans et al.[39, 45]. Finally, samples were diluted using carbon disulfide in a 1:1 volumetric ratio to decrease the viscosity and inhomogeneity of the mixture.

2.5.4.2. GC × GC set-ups

All samples were analyzed on a Thermo Scientific TRACE GC × GC set-up (Interscience, Belgium) equipped with a FID detector, a TOF-MS detector (Interscience, Belgium), a dual-stage cryogenic (liquid CO_2) modulator and a Programmable Temperature Vaporization (PTV) injector (Interscience, Belgium). An MXT-1 (Restek, 60 m, 0.25 mm, 0.25 μm) was used as the first dimension column, while a BPX50 (SGE Analytical Science, 2 m, 0.15 mm, 0.15 μm) was used as the second dimension column. The modulator and both columns were positioned together in a single oven. The PTV temperature was increased from 313 K up to the maximum temperature of 673 K with a rate of 10 K min^{-1}. The initial column temperature was 313 K and was increased up to 643 K at a rate of 2 K min^{-1} where the column was kept isothermally for 600 s. Modulation was carried out on a piece of deactivated column with a set modulation time of 15 s. The scan frequency of the FID was 100 Hz, while the acquisition frequency of the TOF-MS was 30 Hz in a mass range of 15–400 amu. TOF-MS electron impact ionization was 70 eV and the detector voltage was 1700 V. The interface between the GC × GC and the TOF-MS was set at 553 K and the TOF-MS source temperature at 473 K. Optimal helium carrier gas flow of 2.1

ml min^{-1} for FID and 2.6 ml min^{-1} for TOF-MS is calculated according to the method of Beens et al.[40, 46].

2.5.4.3. Data acquisition and quantification

Thermo Scientific's Xcalibur software enabled acquisition and processing of GC × GC-TOF-MS data. For the GC × GC-FID data Thermo Scientific's Chrom-Card data system was used. The raw GC × GC-FID data was exported to a NetCDF file and subsequently processed by GC Image (Zoex Corporation, USA). The obtained peaks were tentatively identified using two independent parameters, *i.e.* cross referencing the measured TOF-MS spectra to the spectra available in the MS libraries[47] and using Kovats retention indices. The blob names and peak volumes were exported as a .csv file which was subsequently processed using an in-house macro file. The quantification procedure described in Supplementary Information was based on the internal standard method developed by Dijkmans et al.[39, 48].

3. RESULTS AND DISCUSSION

3.1. Elemental composition

Elemental compositions of both samples, PFO's obtained from naphtha (hereinafter referred to as N-PFO) and vacuum gas oil steam cracking (hereinafter referred to as V-PFO) are shown in Table 2. Molar hydrogen-to-carbon (H/C) ratios are lower than those reported for asphaltenes from Arabian crude oils[49], however higher compared to those reported for coal tar[50]. This is a first indication of the pronounced aromatic nature of the samples.

Table 2. Comparison of the elemental composition of N-PFO and V-PFO.

Even though naphtha and VGO have significantly different carbon number distribution and chemical composition (see Table 1), their respective PFO's do not differ considerably in H/C ratio. However, a slightly lower value is determined for V-PFO, *i.e.* 0.93, compared to that for N-PFO, *i.e.* 0.95. Due to the low nitrogen and sulfur content in the feedstocks, these elements were on and under the method's detection limit, respectively. On the other hand, oxygen is present in higher amounts, accounting for 1.8 wt.% of the N-PFO and 1.0 wt.% of the V-PFO, respectively. These oxygen amounts suggest the presence of entrained water which was not completely evaporated during the sample preparation step (see section 2.4).

High carbon content and low nitrogen and sulfur content make N-PFO and V-PFO a cheap raw material for production of carbon black[51]. Moreover, a relatively low content of oxygen implies that these fractions are favorable feedstocks for direct liquefaction[52]. Namely, the molar H/C ratio is relatively high and would lead to high quality of products. Similarly, due to the beneficial elemental composition, processes such as Fischer–Tropsch, in which PFO would be steam reformed to synthesis gas and subsequently converted to liquid fuels could be considered.

3.2. SARA fractionation

Fractionation procedure exploiting the difference in solubility of large highly aromatic compounds was used to measure the amount of non-volatile compounds in PFO samples. Fractionation results are dependent on the applied procedure[53] and the nature of the sample. However, results obtained under the same conditions for the samples of similar chemical composition can be compared, and the amount of heavy PAH estimated. Table 3 shows the marked poly-aromatic nature of both samples, *i.e.* the measured amounts of resins, asphaltenes and coke are significant.

Table 3. SARA fractionation results for N-PFO and V-PFO.

The fraction of light compounds evaporated, *i.e.* topping losses, is higher for the N-PFO sample. SARA fractionation analysis indicates that the content of aromatics is higher in the V-PFO. The difference measured according to SARA fractionation is larger due to the higher concentration of heavier poly-aromatics in V-PFO that do not evaporate under reduced pressure during sample topping (see section 2.5.2). Furthermore, the amount of resins is also higher in the V-PFO sample. On the other hand, the content of n-hexane insoluble fraction, defined as asphaltenes and coke (potentially spalled off from the reactor and the TLE) is almost twice higher in N-PFO. Intensified formation of asphaltenes and coke during naphtha cracking can be assigned to the lower dilution and higher cracking temperature[54, 55].

The high concentration of asphaltenes might be the principle disincentive for downstream processing due to potential equipment fouling. However, the content of resins, that serve as a peptizing agents[56], and aromatics is high, making asphaltenes soluble[57, 58]. As V-PFO has a lower asphaltene content and higher amount of aromatics and resins compared to N-PFO, it is a better candidate for further processing. Nevertheless, due to relatively high boiling point of aromatic molecules and resins, the mixture will tend to solidify, thus steam heated lines need to be used for material transfer after the primary fractionation unit.

3.3. Chemical structure

The chemical structure of the hydrocarbon compounds present in PFO is studied in detail using ^{13}C NMR. The spectra obtained for N-PFO and V-PFO are shown in figures, respectively.

Figure 1. ^{13}C NMR spectrum of N-PFO.

Figure 2. ^{13}C NMR spectrum of V-PFO.

The relative quantities of the identified carbon atom types and the lattice parameters used for characterization are shown in Table 4.

Table 4. ^{13}C NMR determined structural and lattice parameters of N-PFO and V-PFO.

Chemical shifts corresponding to phenoxy/phenolic (150-165 ppm), alcohol/ether (50-90 ppm) and methoxy (50-60 ppm) structures are not detected. Similarly, chemical shifts in the range from 165 to 240 ppm are not identified. This confirms the limited content of carboxyl, carbonyl and amide groups. These results indicate that compounds containing carbon/oxygen bonds if present, have a very low concentrations in the studied PFO samples below the method detection limit, *i.e.* 0.3 wt.% of carbon. A more plausible explanation for the oxygen detected using elemental analysis is presence of entrained water. The nature of the feedstock is the dominant factor influencing the high aromatic to aliphatic carbon ratio of the N-PFO. However, the effect is emphasized with lower dilution and higher cracking temperature that further promotes the formation of aromatic cores[40]. Similarly, higher cracking temperatures increase the formation of methylene/methine (22-90 ppm - (50-60) ppm) as opposed to methyl groups (0-22 ppm), which explains the marked difference in abundance between these chemical families for N-PFO. A high aromatic content is confirmed for both samples, accounting for 92.1 wt.% and 89.0 wt.% of N-PFO and V-PFO, respectively. Even though the aliphatic content in V-PFO is higher, the amount of alkyl-substituted aromatic carbon (135-150 ppm) is lower compared to the one of N-PFO. The latter seems unexpected as the presence of non-aromatic carbon is limited, however these two observations indicate that scission of aliphatic side chain bonds is more pronounced during naphtha cracking, as a consequence of higher cracking temperature. Furthermore, by evaluating

the ratio of the aliphatic content and the alkyl-substituted aromatic carbon content, it is possible to estimate the average carbon chain length bonded to the aromatic core. The calculated values of 1.1 for N-PFO and 1.8 for V-PFO are thus in line with the higher cracking severity. Similarly, it is possible to estimate the degree of branching, more specifically aromatic carbon with the alkyl side chain, by dividing the measured amount of alkyl-substituted aromatic carbon with the total aromatic content. This ratio shows that 8 wt.% of N-PFO aromatic carbon and 7 wt.% of V-PFO aromatic carbon have side chain bonds.

3.4. Detailed Chemical Composition by GC × GC

The high boiling point of poly-aromatic compounds implies that not all the compounds present in the PFO mixture will be detectable with gas chromatography. Therefore, the applied GC × GC method is initially evaluated using a standard poly-aromatic hydrocarbon (PAH) mixture (composition given in Table 5).

Table 5. Composition of the standard test mixture.

The standard mixture is analyzed at the conditions subsequently applied for characterization of PFO samples as described in section 2.5.4.2. From the chromatogram shown in Figure 3, it can be concluded that even poly-aromatic molecules with the highest boiling point in the standard mixture, *i.e.* dibenz[a,h]anthracene (797 K) and Indeno[1,2,3-cd]pyrene (809 K), can be detected and quantified. The complete separation of each compound is not achieved. Molecules with the same carbon number, such as benzo[k]fluoranthene and benzo[b]fluoranthene are not separated and the same holds for benzo[ghi]perylene and dibenz[a,h]anthracene. Consequently, such heavy poly-aromatics (five fused aromatic rings) are quantified as a lump of molecules with the same carbon number belonging to the same chemical family.

Figure 3. GC × GC-FID chromatogram of the PAH standard. Numbers correspond to the compounds list in Table 5.

Therefore, the described methodology using GC × GC - TOF-MS and GC × GC - FID enables qualitative and quantitative analysis of part of the PFO samples chemical nature. However, it should be stressed that complete characterization of the samples was not possible. Indeed, the internal standard method shows that 83.7 wt.% of the N-PFO and 92.1 wt.% of the V-PFO are quantified. The higher content of the highly aromatic non-volatile molecules in N-PFO is in agreement with SARA fractionation results which showed 19.5 wt.% and 10.5 wt.% of n-hexane insoluble material for N-PFO and V-PFO, respectively. As shown in the chromatogram for N-PFO in Figures 4 and that for V-PFO in Figure 5, the added internal standard compounds were adequately separated from the other compounds in the resulting chromatograms. This was verified by calculating the bi-dimensional resolution, which should be higher than unity[59] for an adequate separation. In this case the bi-dimensional resolutions were 8.7 for 3-chlorothiophene and 5.0 for 2-chloropyridine. The purpose of adding an internal standard was twofold, on the one hand to determine the quantity of compounds present in the sample and on the other hand to confirm that the homogeneity of the sample is adequate. Known quantities of both standards were used for quantitative analysis and the same results were obtained within experimental precision, which confirms that there was no phase separation within the prepared samples.

Figure 4. GC × GC-FID chromatogram of the N-PFO with separation of molecular families. Numbers correspond to the compounds list in Table 4.

Figure 5. GC × GC-FID chromatogram of the V-PFO with separation of molecular families. Numbers correspond to the compounds list in Table 4.

The nature of compounds in both samples is aromatic, however the carbon number distribution and the relative abundance of molecular families are significantly different. The chemical composition of the samples is compared in terms of molecular family and carbon numbers as shown in Figure 6. Determined compositions are presented in Table S1 and Table S3 with the measurement uncertainty (Table S2 and Table S4) in the Supplementary Information.

Figure 6. Detailed chemical composition by molecular family and carbon number of N-PFO and V-PFO. Molecular families identification and legends can be seen at the top right corner. Results correspond to the average of three repeated injections, and error bars represent twice the standard deviation.

Generally, PFO can be used for isolating basic aromatic chemicals as the carbon content (see Table 2) and the concentration of PAHs (see Table 6) is similar to the one reported for traditionally used coal tar[50]. Extraction of diaromatics is particularly interesting as they are the most abundant molecules in both samples, present in similar quantities, *i.e.* 28.6 wt.% for N-PFO and 27.8 wt.% for V-PFO. The concentration of naphthalene, which is considered as a valuable intermediate[60] in the chemical industry, is 12.5 wt.% in N-PFO, thus higher compared to the concentration in coal tar. Additionally, PFO does not contain phenols and benzo[b]thiophene which are usual contaminants after primary distillation of coal tar[60]. Furthermore, production of solvents, heat transfer oils, heat-resistant polyester fibers and pharmaceutical intermediates requires C_{11}-C_{13} diaromatics, which are present in considerable quantities in both N-PFO and V-PFO (see Figure 6). However, due to the normal and wide distribution of molecules with side chains in V-PFO, separation of pure chemicals is not obvious.

Table 6. Comparison of PAHs concentration in N-PFO and V-PFO.

N-PFO is richer in smaller molecules, such are naphthenoaromatics (18.6 wt.%) than V-PFO (9.7 wt.%). The measured amount of monoaromatics is similar, *i.e.* 16.4 wt.% and 16.9 wt.% for N-PFO and V-PFO, respectively. Nonetheless, it should be noted that direct comparison of aromatic compounds with low boiling point, *i.e.* molecules with carbon number from C_6 to C_9 should be done with care because of the partial evaporation of these molecules during the sample preparation step (see section 2.4). V-PFO has a higher concentration of molecules belonging to the heavier molecular families. The most noticeable differences arise from the amount of triaromatics with a concentration of 14.8 wt.% and 5.6 wt.% for V-PFO and N-PFO, respectively. Similarly, the concentration of naphthenotriaromatics and tetraaromatics in V-PFO, 4.4 wt.% and 4.2 wt.%, respectively, is higher compared to the concentrations in N-PFO, 1.5 wt.% and 1.5 wt.%, respectively.

Even though the carbon number distribution varies for the same molecular family for different samples and for different molecular families within the same sample, some patterns can be recognized. A normal distribution of molecules within each molecular family is clearly visible for the V-PFO. The aliphatic side chains bonded to the aromatic core, *i.e.* di-, tri- and tetraaromatics, and cores that are not completely aromatized, *i.e.* naphtheno-, naphthenodi- and naphthenotriaromatics, are thus only mildly cracked. On the other hand, the purely aromatic molecules, *e.g.* naphthalene for diaromatics, phenanthrene and anthracene for triaromatics, are present in the highest concentration in N-PFO. Furthermore, the concentration of compounds with a longer side chain gradually decreases within these two families. A similar trend is found for tetraaromatics, however these compounds are tentatively identified due to the increased number of isomers. These findings support the conclusion that both the nature of the feedstock

and the cracking temperature affect the ratio between aromatic and aliphatic carbon in the PFO as concluded from ^{13}C NMR results.

The high content of poly-aromatic molecules reduces the stability and furthermore increases the viscosity making utilization of PFO as industrial fuel challenging. The drawbacks can be overcome by thermal processing, *e.g.* visbreaking or coking, where PFO would be converted to gas and lower viscosity liquid product. Production of gas would be favored during conversion of V-PFO due to cracking of plentifully present aliphatic carbon bonded to aromatic and naphthenic structures. On the other hand, the gas oil product would be favored during conversion of N-PFO as a result of higher concentration of lower boiling point compounds, primarily naphthenoaromatics. Poly-aromatic molecules would, however, lead to the formation of large radicals that are coke formation precursors[61], therefore coke formation would be substantial making the process less attractive. Similar issues can be encountered during thermal catalytic cracking due to extensive fouling on the metal catalyst[7, 61].

On the other hand, the abundance of poly-aromatics (see Table 6), *i.e.* PAHs makes blending of PFO with other petroleum streams not straightforward. More specifically, PAHs are recognized as air and food pollutants[62], thus their maximal allowable concentration in petroleum products is regulated[63]. Thereby, the quality of the PFO should be increased through hydro-processing before blending. Hydrotreating and hydrocracking processes would decrease the amount of poly-aromatics and heavy naphthenoaromatic molecules, while increasing the content of monoaromatics[64] and saturates in the product stream[65]. The higher content of smaller molecules in N-PFO, monoaromatics and naphthenoaromatics, would result in lower boiling point products, however the treatment could be economically unjustifiable due to the low amount of PFO

produced during naphtha steam cracking. Nevertheless, the high V-PFO yields suggests hydrotreating or hydrocracking as a possible processing steps for stream valorization.

These detailed compositional characterization results are the basis for assessing exploitation possibilities and setting guidelines for process design. However, use of PFO as a feedstock for the production of valuable chemicals or petroleum products primarily depends on economical evaluation of conversion processes and regional market demands.

4. CONCLUSIONS

A variety of complementary analytical techniques have been used for improving the understanding of the composition of the heaviest reaction products formed during steam cracking of naphtha and VGO. Elemental compositions show relatively low molar H/C ratios, *i.e.* 0.95 for N-PFO and 0.93 for V-PFO, which are lower than the ones typically reported for the asphaltene fraction in Arabian crude oil. The high aromatic content of the produced fractions is confirmed by NMR results, which shows the particularly large aromaticity of the PFO produced during naphtha cracking. The lower dilution ratio and higher temperatures during naphtha compared to VGO cracking promotes formation of heavier poly-aromatic cores and cracking of aliphatic chains. The latter is indicated by the average aliphatic carbon chain length bonded to the aromatic core. On the other hand, the increased presence of heavy aromatic cores is verified through SARA fractionation that shows a larger concentration of n-hexane insolubles, *i.e.* asphaltenes and coke, in N-PFO (19.5 wt.%) compared to V-PFO (10.3 wt.%). Due to the significant concentration of n-hexane insolubles, so-called asphaltenes and coke, it is not possible to completely characterize samples using GC × GC. The optimized GC × GC method enables quantitative characterization of heavy poly-aromatic with boiling point up to 809 K.

Diaromatics are the most abundant molecular families in both PFO's with concentrations up to 29 wt.%. Also naphthenoaromatics are present in significant concentrations in N-PFO (19 wt.%), while triaromatics are more characteristic for V-PFO (15 wt.%) because of the larger quantities of these tricyclics in the original feed. These aromatic molecules together with asphaltenes contribute to the fouling tendency of the PFO, thus hydro-conversion is required for further valorization of PFO either as a feedstock or as a fuel.

ASSOCIATED CONTENT

Procedure for calculation of the mass fractions of the detected compounds by GC × GC-FID/TOF-MS is described in the Supplementary Information. Moreover, the composition of both N-PFO and V-PFO expressed by molecular family and carbon number is reported in Table S1 and Table S3, respectively. Standard deviations of the GC × GC-FID measurements are given in Table S2 and Table S4. Finally, an interested reader can find a schematic description of the pilot plant steam cracker in Figure S1 of Supplementary Information.

AUTHOR INFORMATION

Corresponding Author

*Kevin M. Van Geem

Laboratory for Chemical Technology (LCT), Ghent University

Technologiepark 918, B-9052, Ghent Belgium

Tel.:+3292645677

E-mail address: Kevin.VanGeem@Ugent.be

Notes

The authors declare no competing financial interest.

Author Contributions

The manuscript was written through contributions of all authors. All authors have given approval to the final version of the manuscript.

SAFETY

Do not forget that working with poly-nuclear aromatic hydrocarbons, dichloromethane, carbon disulfide, deuterated chloroform and n-hexane can be extremely hazardous, thus samples should be prepared and kept in well-ventilated areas.

ACKNOWLEDGMENTS

This work was supported by the 'Long Term Structural Methusalem Funding by the Flemish Government' and the European Union Horizon H2020 Programme (H2020-SPIRE-04-2016) under grant agreement n°723706.

ABBREVIATIONS

PFO	Pyrolysis Fuel Oil
VGO	Vacuum Gas Oil
N – PFO	Naphtha Pyrolysis Fuel Oil
V – PFO	Vacuum Gas Oil Pyrolysis Fuel Oil
GC × GC	Comprehensive Two Dimensional Gas Chromatography
NMR	Nuclear Magnetic Resonance
FID	Flame Ionization Detector
TOF – MS	Time-of-Flight Mass Spectrometer

1	H/C	Molar Hydrogen-to-Carbon ratio
2	PAH	Poly-nuclear Aromatic Hydrocarbons
3	TLE	Transfer Line Heat Exchanger
4	CDCl3	Deuterated Chloroform
5	DCM	Dichloromethane
6	SARA	Saturates, Aromatics, Resins and Asphaltenes
7	DIP – MS	Direct Insertion Probe-Mass Spectrometry
8	FT – ICR – MS	Fourier Transform Ion Cyclotron Resonance Mass Spectrometry
9	HPLC	High-performance liquid chromatography
10	CHNS & O	Carbon, Hydrogen, Nitrogen, Sulfur, and Oxygen
11	PINA	Paraffins, Isoparaffins, Naphthenes, Aromatics
12	EA	Elemental Analyzer
13	MPLC	Mid-pressure Liquid Chromatography
14	FAA	Fraction of Aromatic carbons with Attachments
15	Cn’	Average aliphatic Carbon chain length

16

17 REFERENCES

18 1. Froment, G. F. Kinetics and reactor design in the thermal-cracking for olefins production. *Chem.*
19 *Eng. Sci.* **1992,** 47, (9-11), 2163-2177.
20 2. Lederer, J.; Ohanka, V.; Fulin, P.; Sebor, G.; Blazek, J. A study of industrial pyrolysis of the
21 high-boiling products from hydrocracking of petroleum vacuum distillate. *Fuel* **1994,** 73, (2), 295-
22 299.
23 3. Sebor, G.; Blazek, J.; Lederer, J.; Ricanek, M.; Novak, V. Pyrolysis of high-boiling petroleum
24 fractions. *Fuel* **1992,** 71, (11), 1231-1237.
25 4. Sebor, G.; Blazek, J.; Lederer, J.; Bajus, M. Pyrolysis of high-boiling product fractions from
26 petroleum vacuum distillate hydrocracking. *Fuel Process. Technol.* **1994,** 40, (1), 49-59.

5. Khani, M. R.; Guy, E. D.; Gharibi, M.; Shahabi, S. S.; Khosravi, A.; Norouzi, A. A.; Shokri, B. The effects of microwave plasma torch on the cracking of Pyrolysis Fuel Oil feedstock. *Chem. Eng. J.* **2014,** 237, 169-175.

6. Kim, H. G.; Park, M.; Kim, H.-Y.; Kwac, L. K.; Shin, H. K. Characterization of pitch prepared from pyrolysis fuel oil via electron beam irradiation. *Radiat. Phys. Chem.* **2017,** 135, 127-132.

7. Upare, D. P.; Park, S.; Kim, M. S.; Kim, J.; Lee, D.; Lee, J.; Chang, H.; Choi, W.; Choi, S.; Jeon, Y. P.; Park, Y. K.; Lee, C. W. Cobalt promoted Mo/beta zeolite for selective hydrocracking of tetralin and pyrolysis fuel oil into monocyclic aromatic hydrocarbons. *J. Ind. Eng. Chem.* **2016,** 35, 99-107.

8. Mayani, V. J.; Mayani, S. V.; Lee, Y.; Park, S.-K. A non-chromatographic method for the separation of highly pure naphthalene crystals from pyrolysis fuel oil. *Sep. Purif. Technol.* **2011,** 80, (1), 90-95.

9. Rammler, R. Pyrolysis-theory and industrial practice - Albright, L. F., Crynes, B. L., *Corcoran W.H. Angewandte Chemie-International Edition in English* **1984,** 23, (9), 743-743.

10. Van Geem, K. M.; Reyniers, M. F.; Marin, G. B. Challenges of modeling steam cracking of heavy feedstocks. *Oil & Gas Science and Technology-Revue D Ifp Energies Nouvelles* **2008,** 63, (1), 79-94.

11. Kopinke, F. D.; Bach, G.; Zimmermann, G. New results about the mechanism of TLE fouling in steam crackers. *J. Anal. Appl. Pyrolysis* **1993,** 27, (1), 45-55.

12. Wang, R. W.; Liu, G. J.; Zhang, J. M.; Chou, C. L.; Liu, J. J. Abundances of Polycyclic Aromatic Hydrocarbons (PAHs) in 14 Chinese and American Coals and Their Relation to Coal Rank and Weathering. *Energy & Fuels* **2010,** 24, 6061-6066.

13. Joshi, P. V.; Kumar, A.; Mizan, T. I.; Klein, M. T. Detailed Kinetic Models in the Context of Reactor Analysis: Linking Mechanistic and Process Chemistry. *Energy & Fuels* **1999,** 13, (6), 1135-1144.

14. Ghosh, P.; Jaffe, S. B. Detailed composition-based model for predicting the cetane number of diesel fuels. *Ind. Eng. Chem. Res.* **2006,** 45, (1), 346-351.

15. Flego, C.; Zannoni, C. Direct Insertion Probe-Mass Spectrometry (DIP-MS) Maps and Multivariate Analysis in the Characterization of Crude Oils. *Energy & Fuels* **2013,** 27, (1), 46-55.

16. Flego, C.; Carati, C.; Del Gaudio, L.; Zannoni, C. Direct Mass Spectrometry of tar sands: A new approach to bitumen identification. *Fuel* **2013,** 111, 357-366.

17. Flego, C.; Zannoni, C. Direct Insertion Probe-Mass Spectrometry: A Useful Tool for Characterization of Asphaltenes. *Energy & Fuels* **2010,** 24, 6041-6053.

18. Schoenmakers, P. J.; Oomen, J.; Blomberg, J.; Genuit, W.; van Velzen, G. Comparison of comprehensive two-dimensional gas chromatography and gas chromatography - mass spectrometry for the characterization of complex hydrocarbon mixtures. *J. Chromatogr. A* **2000,** 892, (1-2), 29-46.

19. Zhao, Y.; Hong, B.; Fan, Y. Q.; Wen, M.; Han, X. Accurate analysis of polycyclic aromatic hydrocarbons (PAHs) and alkylated PAHs homologs in crude oil for improving the gas chromatography/mass spectrometry performance. *Ecotoxicol. Environ. Saf.* **2014,** 100, 242-250.

20. Cavagnino, D.; Magni, P.; Zilioli, G.; Trestianu, S. Comprehensive two-dimensional gas chromatography using large sample volume injection for the determination of polynuclear aromatic hydrocarbons in complex matrices. *J. Chromatogr. A* **2003,** 1019, (1-2), 211-220.

21. Phillips, J. B.; Beens, J. Comprehensive two-dimensional gas chromatography: a hyphenated method with strong coupling between the two dimensions. *J. Chromatogr. A* **1999,** 856, (1-2), 331-347.

22. Phillips, J. B.; Xu, J. Z. Comprehensive multidimensional gas-chromatography. *J. Chromatogr. A* **1995,** 703, (1-2), 327-334.

23. Dalluge, J.; Beens, J.; Brinkman, U. A. T. Comprehensive two-dimensional gas chromatography: a powerful and versatile analytical tool. *J. Chromatogr. A* **2003,** 1000, (1-2), 69-108.

24. Dutriez, T.; Courtiade, M.; Thiebaut, D.; Dulot, H.; Bertoncini, F.; Vial, J.; Hennion, M. C. High-temperature two-dimensional gas chromatography of hydrocarbons up to nC(60) for analysis of vacuum gas oils. *J. Chromatogr. A* **2009,** 1216, (14), 2905-2912.

25. Dutriez, T.; Courtiade, M.; Thiebaut, D.; Dulot, H.; Hennion, M. C. Improved hydrocarbons analysis of heavy petroleum fractions by high temperature comprehensive two-dimensional gas chromatography. *Fuel* **2010,** 89, (9), 2338-2345.

26. Boursier, L.; Souchon, V.; Dartiguelongue, C.; Ponthus, J.; Courtiade, M.; Thiebaut, D. Complete elution of vacuum gas oil resins by comprehensive high-temperature two-dimensional gas chromatography. *J. Chromatogr. A* **2013,** 1280, 98-103.

27. Koolen, H. H. F.; Swarthout, R. F.; Nelson, R. K.; Chen, H.; Krajewski, L. C.; Aeppli, C.; McKenna, A. M.; Rodgers, R. P.; Reddy, C. M. Unprecedented Insights into the Chemical Complexity of Coal Tar from Comprehensive Two-Dimensional Gas Chromatography Mass Spectrometry and Direct Infusion Fourier Transform Ion Cyclotron Resonance Mass Spectrometry. *Energy & Fuels* **2015,** 29, (2), 641-648.

28. Stanford, L. A.; Kim, S.; Rodgers, R. P.; Marshall, A. G. Characterization of compositional changes in vacuum gas oil distillation cuts by electrospray ionization Fourier transform-ion cyclotron resonance (FT-ICR) mass spectrometry. *Energy & Fuels* **2006,** 20, (4), 1664-1673.

29. Sugumaran, V.; Biswas, H.; Yadav, A.; Christopher, J.; Kagdiyal, V.; Patel, M. B.; Basu, B. Molecular-Level Characterization of Refinery Streams by High-Resolution Mass Spectrometry. *Energy & Fuels* **2015,** 29, (5), 2940-2950.

30. Chacon-Patino, M. L.; Blanco-Tirado, C.; Orrego-Ruiz, J. A.; Gomez-Escudero, A.; Combariza, M. Y. Tracing the Compositional Changes of Asphaltenes after Hydroconversion and Thermal Cracking Processes by High-Resolution Mass Spectrometry. *Energy & Fuels* **2015,** 29, (10), 6330-6341.

31. Xu, C.; Chen, H. M.; Sugiyama, Y.; Zhang, S. J.; Li, H. P.; Ho, Y. F.; Chuang, C. Y.; Schwehr, K. A.; Kaplan, D. I.; Yeager, C.; Roberts, K. A.; Hatcher, P. G.; Santschi, P. H. Novel molecular-level evidence of iodine binding to natural organic matter from Fourier transform ion cyclotron resonance mass spectrometry. *Sci. Total Environ.* **2013,** 449, 244-252.

32. Muller, H.; Adam, F. M.; Panda, S. K.; Al-Jawad, H. H.; Al-Hajji, A. A. Evaluation of Quantitative Sulfur Speciation in Gas Oils by Fourier Transform Ion Cyclotron Resonance Mass Spectrometry: Validation by Comprehensive Two-Dimensional Gas Chromatography. *J. Am. Soc. Mass. Spectrom.* **2012,** 23, (5), 806-815.

33. Clough, A.; Sigle, J. L.; Jacobi, D.; Sheremata, J.; White, J. L. Characterization of Kerogen and Source Rock Maturation Using Solid-State NMR Spectroscopy. *Energy & Fuels* **2015,** 29, (10), 6370-6382.

34. Kelemen, S. R.; Afeworki, M.; Gorbaty, M. L.; Sansone, M.; Kwiatek, P. J.; Walters, C. C.; Freund, H.; Siskin, M.; Bence, A. E.; Curry, D. J.; Solum, M.; Pugmire, R. J.; Vandenbroucke,

M.; Leblond, M.; Behar, F. Direct characterization of kerogen by x-ray and solid-state C-13 nuclear magnetic resonance methods. *Energy & Fuels* **2007,** 21, (3), 1548-1561.

35. Bagley, S. P.; Wornat, M. J. Identification of Five- to Seven-Ring Polycyclic Aromatic Hydrocarbons from the Supercritical Pyrolysis of n-Decane. *Energy & Fuel*s **2011,** 25, (10), 4517-4527.

36. Bagley, S. P.; Wornat, M. J. Identification of Six- to Nine-Ring Polycyclic Aromatic Hydrocarbons from the Supercritical Pyrolysis of n-Decane. *Energy & Fuels* **2013,** 27, (3), 1321-1330.

37. Poddar, N. B.; Thomas, S.; Wornat, M. J. Polycyclic aromatic hydrocarbons from the co-pyrolysis of 1,3-butadiene and propyne. *Proceedings of the Combustion Institute* **2013,** 34, 1775-1783.

38. Thomas, S.; Wornat, M. J. Polycyclic aromatic hydrocarbons from the co-pyrolysis of catechol and 1,3-butadiene. *Proceedings of the Combustion Institute* **2009,** 32, 615-622.

39. Dijkmans, T.; Djokic, M. R.; Van Geem, K. M.; Marin, G. B. Comprehensive compositional analysis of sulfur and nitrogen containing compounds in shale oil using GC x GC - FID/SCD/NCD/TOF-MS. *Fuel* **2015,** 140, 398-406.

40. Van Geem, K. M.; Pyl, S. P.; Reyniers, M. F.; Vercammen, J.; Beens, J.; Marin, G. B. On-line analysis of complex hydrocarbon mixtures using comprehensive two-dimensional gas chromatography. *J. Chromatogr. A* **2010,** 1217, (43), 6623-6633.

41. Dhuyvetter, I.; Reyniers, M. F.; Froment, G. F.; Marin, G. B.; Viennet, D. The influence of dimethyl disulfide on naphtha steam cracking. *Ind. Eng. Chem. Res.* **2001,** 40, (20), 4353-4362.

42. Ristic, N. D.; Djokic, M. R.; Van Geem, K. M.; Marin, G. B. On-line Analysis of Nitrogen Containing Compounds in Complex Hydrocarbon Matrixes. *J. Vis. Exp.* **2016,** (114).

43. Zhang, Y.; Reyniers, P. A.; Schietekat, C. M.; Van Geem, K. M.; Marin, G. B.; Du, W. L.; Qian, F. Computational fluid dynamics-based steam cracking furnace optimization using feedstock flow distribution. *AlChE J.* **2017**, 63, (7), 3199-3213.

44. Solum, M. S.; Pugmire, R. J.; Grant, D. M. C-13 solid-state NMR of Argonne Premium Coals. *Energy & Fuels* **1989,** 3, (2), 187-193.

45. Toraman, H. E.; Dijkmans, T.; Djokic, M. R.; Van Geem, K. M.; Marin, G. B. Detailed compositional characterization of plastic waste pyrolysis oil by comprehensive two-dimensional gas-chromatography coupled to multiple detectors. *J. Chromatogr. A* **2014,** 1359, 237-246.

46. Beens, J.; Janssen, H.-G.; Adahchour, M.; Brinkman, U. A. T. Flow regime at ambient outlet pressure and its influence in comprehensive two-dimensional gas chromatography. *J. Chromatogr. A* **2005,** 1086, (1), 141-150.

47. NIST. Mass Spectral Library and Other Tools. http://www.chemdata.nist.gov

48. Dijkmans, T.; Van Geem, K. M.; Djokic, M. R.; Marin, G. B. Combined Comprehensive Two-Dimensional Gas Chromatography Analysis of Polyaromatic Hydrocarbons/Polyaromatic Sulfur-Containing Hydrocarbons (PAH/PASH) in Complex Matrices. *Ind. Eng. Chem. Res.* **2014,** 53, (40), 15436-15446.

49. Shirokoff, J. W.; Siddiqui, M. N.; Ali, M. F. Characterization of the structure of Saudi crude asphaltenes by X-ray diffraction. *Energy & Fuels* **1997,** 11, (3), 561-565.

50. Blümer, G.-P.; Collin, G.; Höke, H. Tar and Pitch. In Ullmann's Encyclopedia of Industrial Chemistry, *Wiley-VCH Verlag GmbH & Co. KGaA*: **2000**.

51. Jung, M.-J.; Jung, J.-Y.; Lee, D.; Lee, Y.-S. A new pitch reforming from pyrolysis fuel oil by UV irradiation. *Ind. Eng. Chem. Res.* **2015,** 22, 70-74.

52. Omais, B.; Courtiade, M.; Charon, N.; Thiebaut, D.; Quignard, A. Characterization of Oxygenated Species in Coal Liquefaction Products. An Overview. *Energy & Fuels* **2010,** 24, 5807-5816.

53. Rodgers, R. P.; McKenna, A. M., Petroleum Analysis. *Anal. Chem.* **2011**, 83, (12), 4665-4687.

54. Schietekat, C. M.; van Goethem, M. W. M.; Van Geem, K. M.; Marin, G. B. Swirl flow tube reactor technology: An experimental and computational fluid dynamics study. *Chem. Eng. J.* **2014,** 238, 56-65.

55. Schietekat, C. M.; Van Cauwenberge, D. J.; Van Geem, K. M.; Marin, G. B. Computational Fluid Dynamics-Based Design of Finned Steam Cracking Reactors. *AlChE J.* **2014,** 60, (2), 794-808.

56. Wiehe, I. A.; Liang, K. S. Asphaltenes, resins, and other petroleum macromolecules. *Fluid Phase Equilib.* **1996,** 117, (1-2), 201-210.

57. Lestina, T. G.; Zettler, H. U. Crude Oil Fouling Research: HTRI's Perspective. *Heat Transfer Eng.* **2014,** 35, (3), 217-223.

58. Fan, Z. M.; Rahimi, P.; McGee, R.; Wen, Q.; Alem, T. Investigation of Fouling Mechanisms of a Light Crude Oil Using an Alcor Hot Liquid Process Simulator. *Energy & Fuels* **2010,** 24, 6110-6118.

59. Giddings, J. C. Concepts and comparisons in multidimensional separation. *HRC CC J.* **1987,** 10, (5), 319-323.

60. Collin, G.; Höke, H.; Greim, H. Naphthalene and Hydronaphthalenes. In Ullmann's Encyclopedia of Industrial Chemistry, *Wiley-VCH Verlag GmbH & Co. KGaA*: **2000**.

61. Sawarkar, A. N.; Pandit, A. B.; Samant, S. D.; Joshi, J. B. Petroleum residue upgrading via delayed coking: A review. *Can. J. Chem. Eng.* **2007,** 85, (1), 1-24.

62. Ravindra, K.; Sokhi, R.; Van Grieken, R. Atmospheric polycyclic aromatic hydrocarbons: Source attribution, emission factors and regulation. *Atmos. Environ.* **2008,** 42, (13), 2895-2921.

63. Parliament, T. E., Directive 2009/30/EC. In **2009**; Vol. 2009/30/EC.

64. Upare, D. P.; Park, S.; Kim, M. S.; Jeon, Y. P.; Kim, J.; Lee, D.; Lee, J.; Chang, H.; Choi, S.; Choi, W.; Park, Y. K.; Lee, C. W. Selective hydrocracking of pyrolysis fuel oil into benzene, toluene and xylene over CoMo/beta zeolite catalyst. *J. Ind. Eng. Chem.* **2017,** 46, 356-363.

65. Dutriez, T.; Courtiade, M.; Thiebaut, D.; Dulot, H.; Borras, J.; Bertoncini, F.; Hennion, M. C. Advances in Quantitative Analysis of Heavy Petroleum Fractions by Liquid Chromatography-High-Temperature Comprehensive Two-Dimensional Gas Chromatography: Breakthrough for Conversion Processes. *Energy & Fuels* **2010,** 24, 4430-4438.

Table 1. Elemental composition, molecular family mass percentage and boiling point curve of naphtha and VGO.

Elemental Analysis	naphtha	VGO	ASTM-D1160 (K)	naphtha	VGO
Carbon (wt.%)	82.8 ± 0.06	87.62 ± 0.06	0%	296	400
Hydrogen (wt.%)	17.2 ± 0.05	12.3 ± 0.07	5%	316	527
Nitrogen (wt.%)	<0.01[a]	<0.01[a]	10%	319	548
Sulfur (wt.%)	<0.01[a]	0.08 ± 0.02	20%	322	575
Oxygen (wt.%)	<0.01[a]	<0.01[a]	30%	326	592
H/C (mol/mol.)	2.49 ± 0.01	1.68 ± 0.01	40%	330	609
GC × GC	naphtha	VGO	50%	334	622
paraffins (wt.%)	36.40 ± 0.16	23.92 ± 0.31	60%	339	634
isoparaffins (wt.%)	38.85 ± 0.07	24.25 ± 0.61	70%	345	646
cycloalkanes (wt.%)	20.71 ± 0.04	17.60 ± 0.17	80%	352	661
aromatics (wt.%)	4.04 ± 0.02	33.33 ± 0.31	90%	360	675
bio-markers (wt.%)	<0.01[a]	0.91 ± 0.02	95%	367	688
Carbon number	4 - 9	8-35	100%	371	740

a) below the detection limit of the method

Table 2. Comparison of the elemental composition of N-PFO and V-PFO.

	N-PFO	V-PFO	Coal tar[50]	Saudi Arabian asphaltenes[49]
Carbon (wt.%)	90.9 ± 0.4	91.8 ± 0.4	90 – 93	83.2 - 85
Hydrogen (wt.%)	7.2 ± 0.1	7.1 ± 0.1	5 – 6	7.2 – 8.28
Nitrogen (wt.%)	0.1 ± 0.03	0.1 ± 0.01	0.6 – 1.2	0.3 – 0.8
Sulfur (wt.%)	< 0.01[a]	< 0.01[a]	0.6 – 1.0	6.3 – 7.2
Oxygen (wt.%)	1.8 ± 0.1	1.0 ± 0.1	1.5 – 2.0	0.5 - 1.1
H/C (mol/mol)	0.95 ± 0.02	0.93 ± 0.02	0.69	1.02 – 1.19

a) below the detection limit of the method

Table 3. SARA fractionation results for N-PFO and V-PFO.

	N-PFO	V-PFO
Topping loss, wt.%	53.9 ± 0.5	28.7 ± 0.1
Saturates, wt.%	0.9 ± 0.1	0.5 ± 0.1
Aromatics, wt.%	16.5 ± 1.4	43.3 ± 0.2
Resins, wt.%	8.7 ± 0.5	14.1 ± 0.2
Asphaltenes & coke, wt.%	19.5 ± 0.5	10.3 ± 0.2

Reported values correspond to the average of two measurement, the associated uncertainty indicates the difference with respect to the average.

Table 4. ^{13}C NMR determined structural and lattice parameters of N-PFO and V-PFO.

Structural parameter	chemical shift range (ppm)	N-PFO (wt.%)	V-PFO (wt.%)
aromatic (fa')	90-165	92.07 ± 0.07	89.01 ± 0.28
carboxyl/carbonyl/amide (fa^C)	165-240	<0.3[a]	<0.3[a]
phenoxy/phenolic (fa^P)	150-165	<0.3[a]	<0.3[a]
alkyl-substituted aromatic, biaryl (fa^S)	135-150	7.14 ± 0.40	6.07 ± 0.27
aliphatic (fal)	0-90	7.93 ± 0.07	10.99 ± 0.29
methylene/methine (fal^H)	22-90 – (50-60)	5.84 ± 0.30	6.05 ± 0.25
methyl (fal*)	0-22	2.10 ± 0.37	4.94 ± 0.03
methoxy (fal^{mo})	50-60	<0.3[a]	<0.3[a]
alcohol/ether (fal^O)	50-90	<0.3[a]	<0.3[a]
lattice parameter	definition	N-PFO	V-PFO
fraction of aromatic carbons with attachments (FAA)	$(fa^P+fa^S)/fa'$	0.08	0.07
average aliphatic carbon chain length (Cn')	fal/fa^S	1.11	1.81

Reported values correspond to the average of two measurements, the associated uncertainty indicates the difference with respect to the average.

a) below the detection limit of the method

Table 5. Composition of the standard test mixture.

Assigned number in the chromatogram	Compound name
1	Naphthalene
2	1-Methylnaphthalene
3	2-Methylnaphthalene
4	Acenaphthene
5	Acenaphthylene
6	Fluorene
7	Phenanthrene
8	Anthracene
9	Fluoranthene
10	Pyrene
11	Benzo[a]anthracene
12	Chrysene
13	Benzo[k]fluoranthene
14	Benzo[b]fluoranthene

15		Benzo[a]pyrene
16		Benzo[ghi]perylene
17		Dibenz[a,h]anthracene
18		Indeno[1,2,3-cd]pyrene

Table 6. Comparison of PAHs concentration in N-PFO and V-PFO.

Compound name	N-PFO	V-PFO	Coal Tar[50]
Naphthalene	12.5	3.8	10.0
1-Methylnaphthalene	2.1	2.2	0.7
2-Methylnaphthalene	3.7	3.3	1.5
Acenaphthene	0.4	0.2	0.2
Acenaphthylene	1.7	1.0	2.5
Fluorene	1.1	1.0	1.8
Phenanthrene	1.6	1.4	4.5
Anthracene	0.3	0.4	1.3
Fluoranthene	0.1	0.2	3.0
Pyrene	0.4	0.3	2.0
Chrysene	0.1	0.1	1.0

Results correspond to the average of three repeated injections.

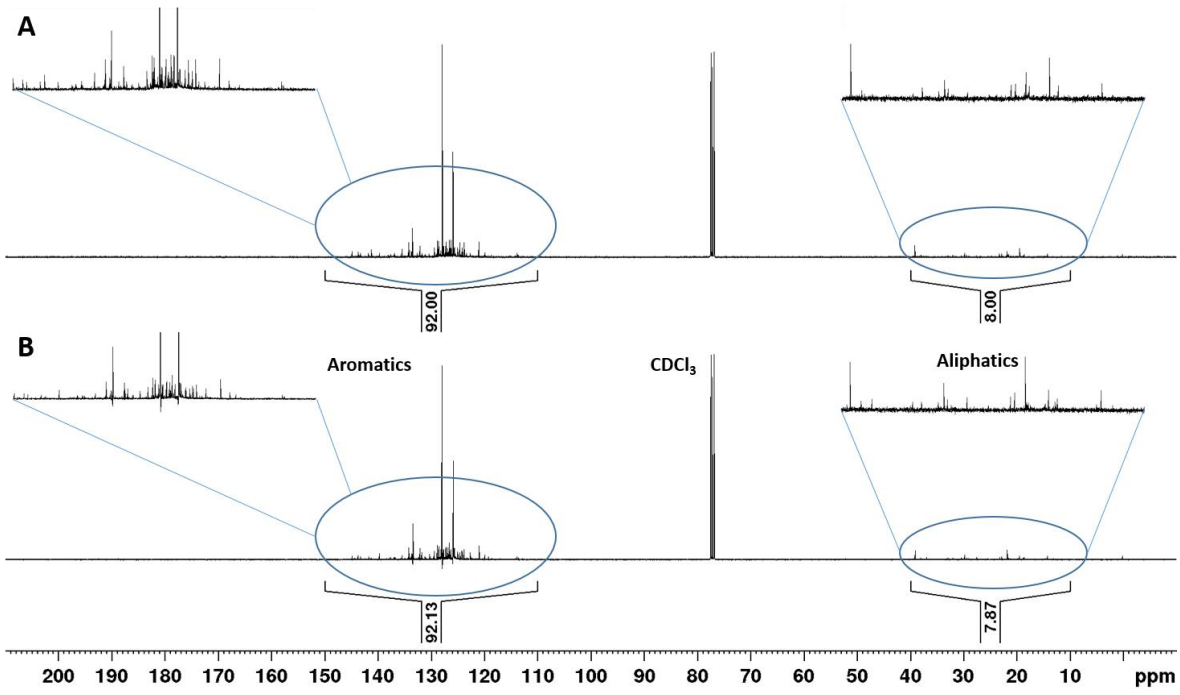

Figure 1. ^{13}C NMR spectrum of N-PFO.

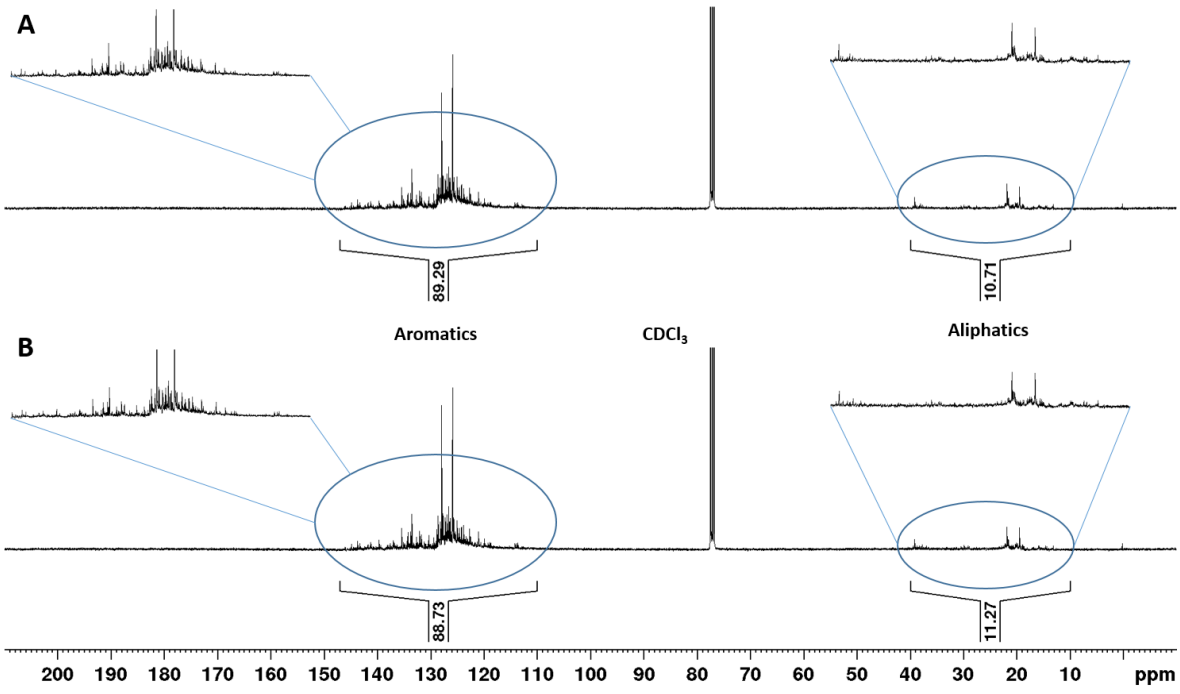

Figure 2. ^{13}C NMR spectrum of V-PFO.

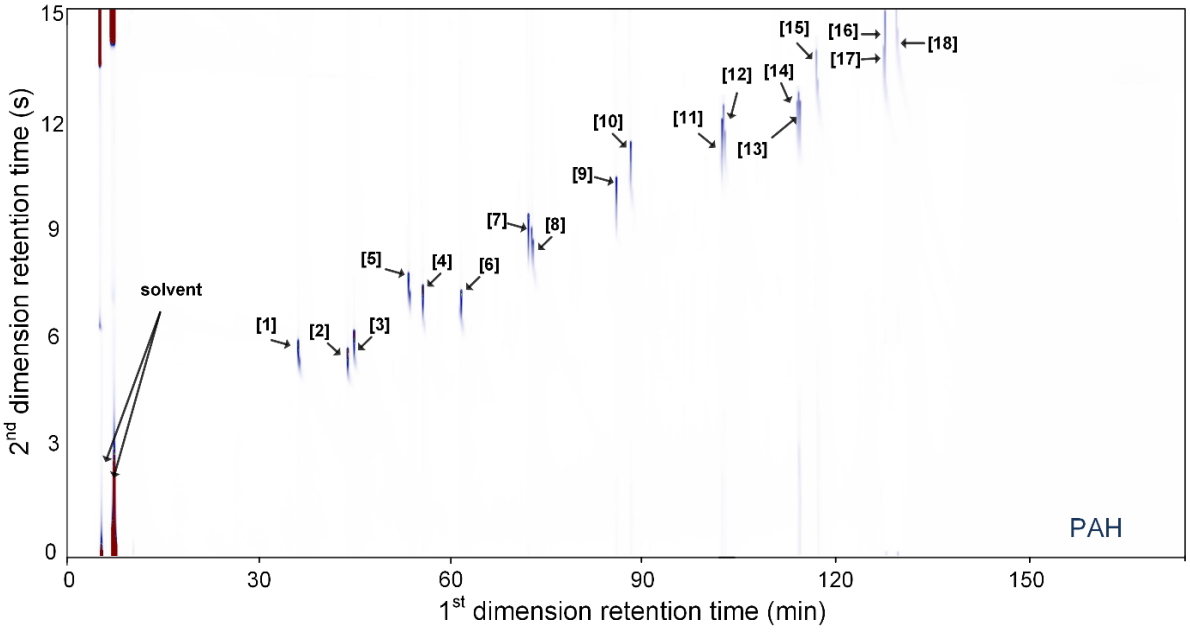

Figure 3. GC × GC-FID chromatogram of the PAH standard. Numbers correspond to the compounds list in Table 5.

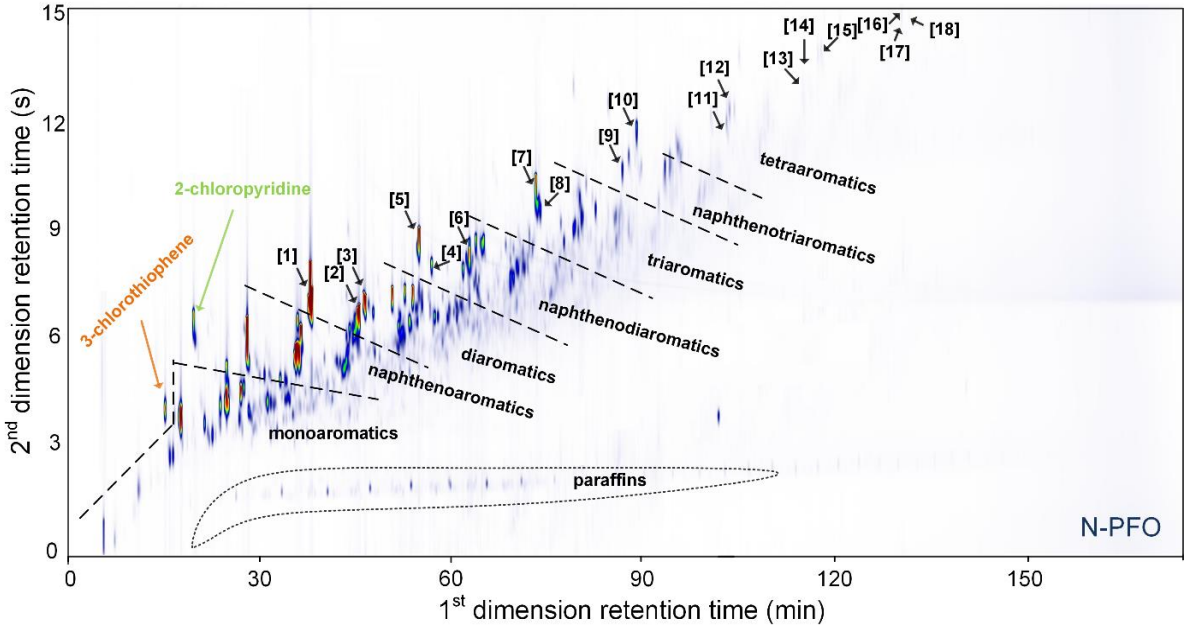

Figure 4. GC × GC-FID chromatogram of the N-PFO with separation of molecular families. Numbers correspond to the compounds list in Table 5.

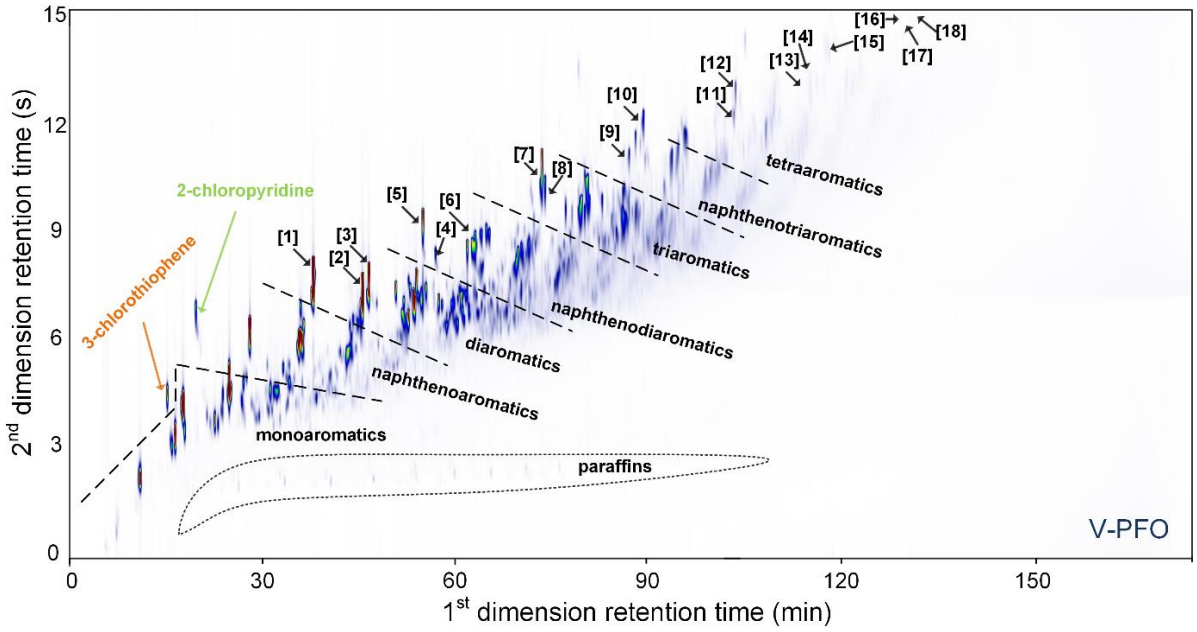

Figure 5. GC × GC-FID chromatogram of the V-PFO with separation of molecular families. Numbers correspond to the compounds list in Table 5.

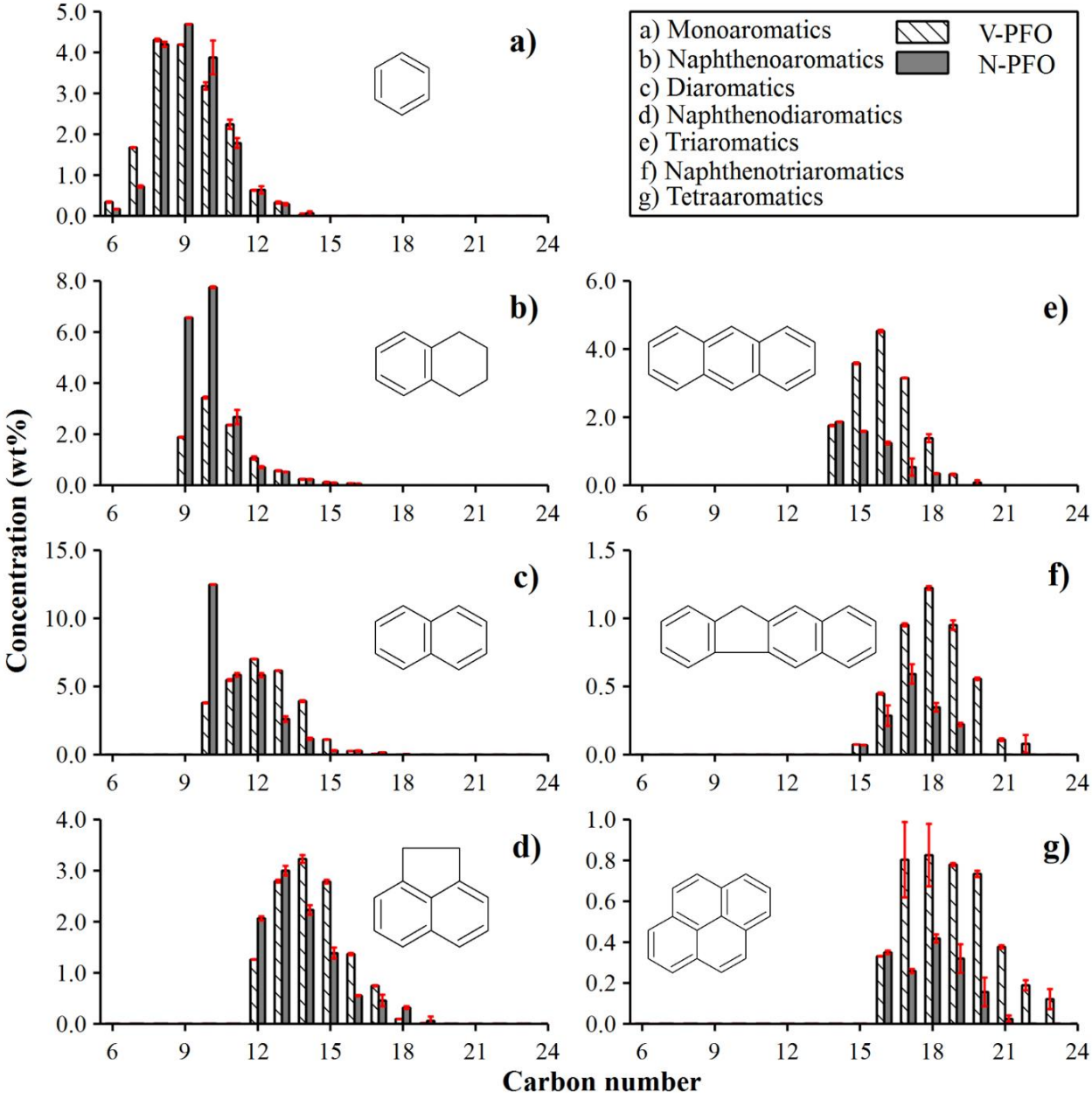

Figure 6. Detailed chemical composition by molecular family and carbon number of N-PFO and V-PFO. Molecular families identification and legends can be seen at the top right corner. Results correspond to the average of three repeated injections, and error bars represent twice the standard deviation.